

# Osculating and neighbour-avoiding polygons on the square lattice

Iwan Jensen\*

Department of Mathematics & Statistics,  
The University of Melbourne, Victoria 3010, Australia

October 26, 2018

## Abstract

We study two simple modifications of self-avoiding polygons. Osculating polygons are a super-set in which we allow the perimeter of the polygon to touch at a vertex. Neighbour-avoiding polygons are only allowed to have nearest neighbour vertices provided these are joined by the associated edge and thus form a sub-set of self-avoiding polygons. We use the finite lattice method to count the number of osculating polygons and neighbour-avoiding polygons on the square lattice. We also calculate their radius of gyration and the first area-weighted moment. Analysis of the series confirms exact predictions for the critical exponents and the universality of various amplitude combinations. For both cases we have found exact solutions for the number of convex and almost-convex polygons.

## 1 Introduction

A self-avoiding polygon (SAP) can be defined as a walk on a lattice which returns to the origin and has no other self-intersections. Generally SAPs are considered distinct up to a translation, so if there are  $p_n$  SAPs of length  $n$  there are  $2np_n$  walks (the factor of two arising since the walk can go in either direction). The enumeration of self-avoiding polygons on various lattices is an interesting combinatorial problem in its own right, and is also of considerable importance in the statistical mechanics of lattice models [16]. Despite strenuous effort this problem has not been solved on any regular two dimensional lattice. However, progress has been made in the study of restricted classes of polygons and many problems have been solved exactly. These include staircase polygons [28, 26, 7, 3, 22], convex polygons [7, 20, 14, 21], row-convex polygons [3, 22], and almost convex polygons [23].

In this paper we study two simple modifications of SAP. Osculating polygons (OP) form a super-set in which we allow the walk to touch at a vertex but not to cross. Neighbour-avoiding polygons (NAP) are only allowed to have nearest neighbour vertices when the adjoining edge is part of the perimeter of the polygon (any two occupied vertices are separated by at least one empty vertex) and they are a sub-set of SAP. See figure 1 for an example of each case. Osculating polygons were introduced in [17] while neighbour-avoiding polygons were studied in

---

\*e-mail: I.Jensen@ms.unimelb.edu.au

[1] as the special limiting case of interacting polygons with infinitely strong repulsion. We use the finite lattice method to count the number of osculating and neighbour-avoiding polygons on the square lattice. We also calculate their radius of gyration and the first and second area-weighted moments. The quantities we consider are: (i) the polygon generating function,  $\mathcal{P}(u) = \sum p_n u^n$ ; (ii)  $k^{\text{th}}$  area-weighted moments of polygons of perimeter  $n$ ,  $\langle a^k \rangle_n$ ; and (iii) the mean-square radius of gyration of polygons of perimeter  $n$ ,  $\langle R^2 \rangle_n$ . These quantities are expected to behave as

$$\begin{aligned} p_n &= B\mu^n n^{\alpha-3}[1 + o(1)], \\ \langle a^k \rangle_n &= E^{(k)} n^{2k\nu}[1 + o(1)], \\ \langle R^2 \rangle_n &= Dn^{2\nu}[1 + o(1)], \end{aligned} \tag{1}$$

where  $\mu = u_c^{-1}$  is the reciprocal of the critical point of the generating function, and  $\alpha = 1/2$  and  $\nu = 3/4$  are known exactly [25], though non-rigorously, in the case of the honeycomb lattice. Very firm evidence exists from previous numerical work that the exponent  $\alpha$  is universal and thus equals  $1/2$  for all two dimensional lattices [13, 10, 17]. The value  $\nu = 3/4$  is likewise well supported by the existing numerical evidence [27, 13, 11, 19]. It is also known [5] that the SAP amplitude combination  $E^{(1)}/D$  is universal, and that

$$BD = \frac{5}{32\pi^2} \sigma a_0, \tag{2}$$

where  $a_0$  is the area per site and  $\sigma$  is an integer such that  $p_n$  is non-zero only if  $n$  is divisible by  $\sigma$ . For the square lattice  $a_0 = 1$  and  $\sigma = 2$ . These predictions have been confirmed numerically for SAP on many different lattices [5, 24, 19]. We would expect the universality of these amplitude combinations to hold for NAP. What happens for OP is not immediately clear. The derivation in [5] relies on the self-avoidance and indeed the universality does not extend to trailgons (trails are walks which are allowed to share a vertex but *not* an edge) which are a super-set of OP. We shall provide compelling evidence that with a suitable definition of the radius of gyration the universality does extend to OP.

Any polygon has a minimal bounding rectangle. A polygon is said to be convex if its perimeter has the same length as its minimal bounding rectangle. More generally one can classify polygons according to their concavity  $c$ , with the perimeter of a polygon of concavity  $c$  exceeding the length of the minimal bounding rectangle by  $2c$ . For both OP and NAP we have found exact solutions for the generating functions for convex and almost-convex ( $c = 1$ ) polygons.

In the next section we briefly describe the generalisation of the finite lattice method required in order to enumerate OP and NAP. The results of the analysis of the series are presented in Section 3. Exact results for the generating functions for convex and almost-convex OP and NAP are presented in Section 4.

## 2 Enumeration of polygons

The method used to enumerate OP and NAP on the square lattice are simple generalisations of the method devised by Enting [8] in his pioneering work and includes the significant enhancements employed in previous work [18, 19]. The general method has been described in

some detail in these papers and for this reason we shall be very brief and only give the absolute essential information.

The first terms in the series for the polygon generating function can be calculated using transfer matrix techniques to count the number of polygons in rectangles  $W + 1$  edges wide and  $L + 1$  edges long. The transfer matrix technique involves drawing a boundary through the rectangle intersecting a set of  $W + 2$  edges. For each configuration of occupied or empty edges along the boundary we maintain a (perimeter) generating function for partially completed polygons. Polygons in a given rectangle are enumerated by moving the boundary so as to add one site at a time as shown in figure 3. Configurations are represented by a set of edge states  $\{n_i\}$ , where

$$n_i = \begin{cases} 0 & \text{empty edge,} \\ 1 & \text{lower part of loop,} \\ 2 & \text{upper part of loop.} \end{cases} \quad (3)$$

Reading configurations from the bottom edge up, the partially completed polygon in figure 3 is encoded as  $\{1010210202\}$  before the move of the boundary line and  $\{1010000202\}$  after the move. The rules for updating the partial generating functions are described in [8] and we refer the interested reader to this paper for further details.

In the following sections we shall briefly outline the changes required in order to enumerate OP and NAP.

## 2.1 Osculating polygons

OP are allowed to have vertices on which the perimeter touch but no crossing takes place. Obviously such vertices are of degree 4 and in terms of the updating rules are vertices with two incoming and outgoing occupied edges. The possibilities are thus that the incoming edges are in states  $\{11\}$ ,  $\{22\}$ ,  $\{21\}$ , or  $\{12\}$ . The first three of these are essentially identical in that they permit similar outputs. From  $\{11\}$  we can produce the outputs  $\{00\}$  (with appropriate relabelling of the remainder of the configuration as per the original SAP problem) and the two additional outputs  $\{11\}$  and  $\{12\}$ . The three possibilities are illustrated in figure 2 and correspond to cases where, respectively, the edges are joined with no further action, bounce of one-another, or are joined and a new loop is inserted. The case  $\{12\}$  is special in that joining the edges results in a closed loop and thus the formation of a separate component. This is only allowed provided there are no other occupied edges and the result is a valid polygon. This leaves us just with the ‘bouncing’ output  $\{12\}$  as illustrated in figure 2. The updating rules for the transfer-matrix algorithm are summarised in Table 1.

At this point it is pertinent to give some detail about our calculation of the radius of gyration. The general algorithm was described in [19] but we made some changes to accommodate the degree 4 vertices of OP. In the basic definition [27] one calculates the radius of gyration of the vertices contained in the perimeter of the polygon. The problem is how to count the degree 4 vertices of OP. We have chosen to rely on the definition of polygons as walks which return to the starting point. Viewed in this light it is natural to count degree 4 vertices twice, once for each time the walk visits the vertex. This makes the necessary generalisation of the algorithm quite simple and no further details will be given. As we shall see when analysing the series this definition also ensures that the amplitude combinations  $BD$  and  $E^{(1)}/D$  remain universal.

We calculated the number of OP with perimeter up to  $n = 90$  and their radius of gyration and area-weighted moment up to  $n = 82$ .

## 2.2 Neighbour-avoiding polygons

The generalisations to NAP is a little more involved, but the required generalisation has been described in some detail in [1] and we shall thus be brief. In order to ensure the nearest neighbour avoidance we have to encode some extra information in the boundary configuration. Essentially we introduce an extra state ‘3’, which labels an empty edge along which a contact could occur, i.e. an empty edge next to the perimeter of the polygon. As an illustration consider again the partially completed polygon in figure 3. This is now encoded as {1013213202} before the move of the boundary line and {1013333202} after the move. We are not allowed to occupy any edge adjacent to an edge in state ‘3’ since this would result in an illegal contact. This restriction means the updating rules can depend not only on the edges in the kink itself (as for SAP and OP) but also on the states of nearby edges. The rules for allowed transition of the boundary line in the transfer-matrix algorithm are summarised in Table 2.

We calculated the number of NAP with perimeter up to  $n = 86$  and their radius of gyration and area-weighted moment up to  $n = 82$ .

## 3 Analysis of series

The series have exponentially growing coefficients, with sub-dominant term given by a critical exponent. The generic behaviour is  $G(u) = \sum_n g_n u^n \sim (1 - u/u_c)^{-\xi}$ , and hence the coefficients of the generating function  $g_n \sim \mu^n n^{\xi-1}$ , where  $\mu = 1/u_c$ . To obtain the singularity structure of the generating functions we used the numerical method of differential approximants [15]. Combining the relationship given above between the coefficients in a series and the critical behaviour of the corresponding generating function with the expected behaviour Eq. (1) of the mean-square radius of gyration and moments of area yields the following prediction for their generating functions:

$$\mathcal{R}_g^2(u) = \sum_n p_n \langle R^2 \rangle_n u^n = \sum_n r_n u^n \sim R(u)(1 - u/u_c)^{-(\alpha+2\nu)}, \quad (4)$$

$$\mathcal{P}^{(k)}(u) = \sum_n p_n \langle a^k \rangle_n u^n = \sum_n a_n^{(k)} u^n \sim a^{(k)}(u)(1 - u/u_c)^{2-(\alpha+2k\nu)}, \quad (5)$$

As stated previously the exponent  $\alpha = 1/2$  while  $\nu = 3/4$ . Since the series only contain even terms and the smallest polygon has size 4, we actually analyse the series  $P(x) = \sum_n p_{2n+4} x^n$ , and so on, and obtain estimates for  $x_c = u_c^2 = 1/\mu^2$ .

Our use of differential approximants have been described in detail in [18, 19] so suffice to say that estimates for the critical points and exponents are obtained by averaging over many separate approximants each using most of the series coefficients and yielding individual estimates. A very rough and not necessarily reliable error estimate is obtained from the spread among the approximants.

Next we turn our attention to the ‘‘fine structure’’ of the asymptotic form of the coefficients. In particular we are interested in obtaining accurate estimates for the amplitudes  $B$ ,  $D$  and  $E^{(1)}$ . We do this by fitting the coefficients to the assumed form (1). The asymptotic form of the coefficients  $p_n$  of the SAP generating function was studied in detail previously [6, 18]. As argued in [6] there is no sign of non-analytic corrections-to-scaling exponents to the polygon generating function and one therefore finds that

$$p_n = \mu^n n^{-5/2} \sum_{k=0} a_k/n^k. \quad (6)$$

This form was confirmed with great accuracy in [18]. For the radius of gyration coefficients we found in [19] that we had to take direct account of the correction-to-scaling exponent  $\Delta = 3/2$  which leads to the asymptotic form

$$r_n = \mu^n n [BD + \sum_{k=0} a_k / n^{k/2}]. \quad (7)$$

Alternative we could also fit to the form

$$r_n/p_n = n^{7/2} [D + n^{5/2} \sum_{k=0} a_k / n^{k/2}]. \quad (8)$$

Asymptotic forms similar to those above also hold for the area-moment coefficients after the appropriate change of the leading exponent.

### 3.1 Osculating polygons

In Table 3 we have listed estimates for the critical point and exponents obtained from second and third order differential approximants to the polygon generating function, radius of gyration, and first area moment series. It is obvious that the OP generating function has an exponent consistent with the exact values  $2 - \alpha = 3/2$ , as we would expect. It is equally clear that the first moment as expected has a logarithmic singularity thus confirming  $\nu = 3/4$ . From the polygon series we also find an accurate estimate for the critical point  $x_c = 0.139445164(3)$ . The estimates for the exponent of the radius of gyration series differs slightly from the expected value of  $-(\alpha + 2\nu) = -2$ . However, the estimates obtained from this series are also much less accurate than those from the other series and the value  $-2$  can certainly not be ruled out. In order to try to obtain a more accurate estimate of  $x_c$  and resolve the discrepancy of the radius of gyration series we look in greater detail at estimates from the individual differential approximants. In figure 4 we have plotted estimates of the critical exponents vs. the corresponding critical points. From the data in the left panel we see an essentially linear relationship between estimates for the exponent  $2 - \alpha$  and  $x_c$ , We notice that the exponent attains its expected value  $3/2$  when  $x_c = 0.1394451660(5)$ , which we take as our final estimate for  $x_c$ , and we thus find  $\mu^O = 2.677924128(5)$ . As one would expect  $\mu^O$  is larger than the connective constant  $\mu = 2.63815853034(10)$  for SAP. From the data for the radius of gyration we notice that the curve traced by estimates comes very close to crossing through the point given by the expected exponent value and the value for  $x_c$  just obtained. We also note that in a similar plot using second order approximants the curve was further removed from this point. We take this as firm evidence that given a sufficiently long series and high enough order approximants any discrepancy between the behaviour of the actual estimates and the expected behaviour would be completely resolved.

Having confirmed that the exponents have their expected values and obtained a very accurate estimate for  $x_c$ , we turn our attention to the leading amplitudes. First we note that the expected asymptotic form given in Eq. (6) is completely confirmed by repeating the analysis carried for the SAP case [18]. The results for the leading amplitude are displayed in figure 5. We notice that all fits appear to converge to the same value as  $n \rightarrow \infty$ , and that, as more and more correction terms are added to the fits the estimates exhibits less curvature and that the slope become smaller (although the fits using 9 terms are a little inconclusive). This is very strong evidence that Eq. (6) indeed is the correct asymptotic form of  $p_n$ . We estimate that  $B = 0.6355995(10)$ . The corresponding plots for the amplitude combination  $BD$ , obtained

from the radius of gyration series, clearly show that these estimates are consistent with the exact value  $BD = 5/16\pi^2$ , and we thus estimate  $D = 0.04981575(15)$ . A similar analysis of the area-moment series yields the estimate  $E^{(1)} = 0.12520(1)$ . From this we find the amplitude ratio  $E^{(1)}/D = 2.51326(20)$  in remarkable agreement with the estimate  $E^{(1)}/D = 2.51326(3)$  from the SAP series [19].

### 3.2 Neighbour-avoiding polygons

Table 4 lists estimates for the critical point and exponents for the NAP series. Albeit the accuracy of these estimates is somewhat poorer than before there can be no doubt that the exponent estimates are consistent with the expected exact values. Again we use a plot of  $2-\alpha$  vs.  $x_c$  to obtain the improved estimate  $x_c = 0.1864580(5)$  and thus  $\mu^{\text{NA}} = 2.315845(4)$ . As expected this connective constant is smaller than the SAP counter-part. We note that the corresponding value for the walk generating function  $u_c = \sqrt{x_c} = 0.4318078(6)$  is in full agreement with the unbiased estimate  $u_c = 0.43180(2)$  given in [1], but quite a bit larger than the same papers biased estimate  $u_c = 0.4317925(1)$ . The only possible explanation we can think off for this discrepancy is that perhaps the exponent used in biasing was wrong. Cardy [4] predicted that excluding walks with parallel nearest-neighbour steps should result in a change in the exponent  $\gamma$  of the walk generating function. Numerical studies confirmed a slight change in exponent for Manhattan lattice SAW [2] (by its very definition the Manhattan lattice does not allow any parallel nearest-neighbour steps). Clearly neighbour-avoiding walks have no nearest-neighbour steps at all. In [1] the authors used the usual SAW exponent  $\gamma = 43/32$ , which thus could be the wrong choice for neighbour-avoiding walks. In fact one might see the discrepancy with the biased estimate for  $u_c$  as further evidence that there is a change in the exponent  $\gamma$  for walks with no parallel nearest-neighbour steps.

For NAP the analysis of the radius of gyration and area-moment series confirm the universality of  $BD$  and  $E^{(1)}/D$ . Using this and the direct analysis of the polygon series we arrive at the amplitude estimates  $B = 0.36955(5)$ ,  $D = 0.08568(1)$  and  $E^{(1)} = 0.21534(2)$

## 4 Exact results for convex and almost-convex polygons

In section 2 we described how the series expansion for the polygon generating function was calculated by counting the number of polygons spanning various  $W \times L$  rectangles. From this data it is obviously easy to extract the corresponding series for the generating functions for convex polygons with concavity  $c$ . In the following we use these series to calculate the exact generating functions for convex and almost-convex OP and NAP.

Throughout this section we use the variable  $x$  as the conjugate of the semi-perimeter of the polygons. In other words the coefficients of  $x^k$  is the number of polygons of perimeter  $n = 2k$ .

### 4.1 Convex polygons

The generating function for convex osculating polygons (COP) is quite easy to derive. First of all we note that any ordinary convex polygon is a COP. So all we need calculate is the generating function for polygons with at least one osculation. It is not difficult to see that these polygons can be obtained by simple concatenations. In the simplest case we can take a convex polygon whose top right-hand corner is also the corner of the minimal bounding

rectangle and concatenate with a convex polygon whose bottom left-hand coincides with the bounding rectangle (obviously these two types of polygons have identical generating functions). Due to the convexity constraint the only way to get more osculations is by inserting convex polygons where *both* the top right-hand and bottom left-hand corners are shared with the minimal bounding rectangle. Thankfully the generating functions for these types of polygons are already known. The generating function for the first type of polygons was calculated by Lin and Chang [21] and in their honour we shall stick with their notation and call this function  $H(x)$ . The second intermediate type of convex polygons are the well-known and much loved staircase polygons, their generating function is  $S(x)$ . Since we can insert any number of staircase polygons and go along either diagonal of the square lattice we find that the generating function,  $\mathcal{C}^{\text{O}}$ , for convex osculating polygons is

$$\mathcal{C}^{\text{O}}(x) = \mathcal{C}(x) + 2H(x)/(1 - S(x)), \quad (9)$$

where  $\mathcal{C}$  is the generating function for convex polygons.

After inserting the known generating functions

$$\begin{aligned} \mathcal{C}(x) &= x^2(1 - 6x + 11x^2 - 4x^3)(1 - 4x)^{-2} - 4x^4(1 - 4x)^{-3/2}, \\ H(x) &= x^2(1 - 4x)^{-1/2}, \\ S(x) &= (1 - 2x - \sqrt{1 - 4x})/2, \end{aligned}$$

and doing a little arithmetic we find

$$\mathcal{C}^{\text{O}}(x) = x^2(2 - 10x + 14x^2 - 5x^3 - 4x^4)/[(1 - 4x)^2(2 + x)] - x^3(1 + 2x)^2/[(1 - 4x)^{-3/2}(2 + x)]. \quad (10)$$

The generating function,  $\mathcal{C}^{\text{NA}}$ , for convex neighbour-avoiding polygons (CNAP) is simply  $\mathcal{C}^{\text{NA}}(x) = x^2[1 + \mathcal{C}^{\text{O}}(x)]$ . In other words, with the exception of the simplest polygon of size  $n = 4$ , the number of COP is identical to the number of CNAP with four more steps. This means that there should be a simple bijection between COP with perimeter  $n$  and CNAP with perimeter  $n + 4$ . To describe this bijection we need a slightly different way to describe a convex polygon. We can define convex polygons as consisting of four straight lines (one on each side of the minimal bounding rectangle) connected via directed walks, e.g. the left-most line is connected to the top-most line via a walk taking steps only to the right and up and so on. Mutually the directed walks have to respect the general restrictions for a given class of polygons. We can get a contact where the directed walks connect to the straight lines. From this we see that a necessary conditions for a CNAP is that all straight pieces have length at least 2 (it is not sufficient since the mutual neighbour avoidance of the directed walks is not automatically guaranteed). The bijection is now obvious. To go from a COP to a CNAP with 4 more steps we simply extend each straight piece by a single step and to go from a CNAP to a COP we contract each straight piece by a single step. That the first operation takes us from a COP to a CNAP is clear. The convexity is clearly preserved and the extension of the straight pieces ensures that all occupied vertices are separated by an empty vertex and thus the condition on a NAP is fulfilled. That the reverse operation takes us from a CNAP to a COP is perhaps not as obvious. Note however that due to the neighbour avoidance there is at least one empty vertex between any two vertices of the CNAP. So deletion operation can never result in overlapping or crossing of occupied edges, at most we can get an osculation.

## 4.2 Almost-convex polygons

The generating function,  $\mathcal{C}_1(x)$  for almost convex polygons was calculated exactly by Lin [23], who found

$$\mathcal{C}_1(x) = 16x^3A/[(1-x)(1-4x)^{5/2}] + 4x^3B/[(1-x)(1-3x+x^2)(1-4x)^3], \quad (11)$$

where  $A$  and  $B$  are low-order polynomials with integer coefficients:

$$\begin{aligned} A &= 1 - 9x + 25x^2 - 23x^3 + 3x^4, \\ B &= -4 + 56x - 300x^2 + 773x^3 - 973x^4 + 535x^5 - 90x^6 + 24x^7. \end{aligned}$$

Given the close similarity between OP, NAP and SAP it is natural to look for a solution of a form similar to Eq. (11). From the solution to the convex case Eq. (10) one would expect extra factors of  $(2+x)$  to turn up in the denominators. Using standard mathematical software packages it is easy to check for solutions of a form similar to to Eq. (11). In this case we simply make an educated guess for the denominator  $D$  associated with  $B$ , multiply our series for almost-convex polygons with  $D$  and look for a solution of the form  $A + B\sqrt{1-4x}$  by formally expanding this expression and solving for the unknown coefficients in the polynomials  $A$  and  $B$ .

In this manner we found the generating function for almost-convex OP to be

$$\mathcal{C}_1^{\text{O}}(x) = 4x^2A^{\text{O}}/[(2+x)(1-x)(1-4x)^{5/2}] + 4x^2B^{\text{O}}/[(2+x)^2(1-x)^2(1-3x+x^2)(1-4x)^3], \quad (12)$$

where:

$$\begin{aligned} A^{\text{O}} &= 2 - 10x - 10x^2 + 55x^3 + 25x^4 - 17x^5 + 24x^6 + 12x^7, \\ B^{\text{O}} &= -2 + 22x - 70x^2 - 5x^3 + 371x^4 - 521x^5 + 175x^6 - 44x^7 + 101x^8 - 219x^9 - 238x^{10} - 56x^{11}. \end{aligned}$$

Similarly we found the generating function for almost-convex NAP

$$\mathcal{C}_1^{\text{NA}}(x) = 4x^4A^{\text{NA}}/[(2+x)^2(1-x)^2(1-4x)^{5/2}] + 4x^4B^{\text{NA}}/[(2+x)^2(1-x)^2(1-3x+x^2)(1-4x)^3], \quad (13)$$

where:

$$\begin{aligned} A^{\text{NA}} &= 2 - 16x + 22x^2 + 79x^3 - 149x^4 - 86x^5 + 89x^6 + 36x^7 - 38x^8 - 20x^9, \\ B^{\text{NA}} &= -2 + 26x - 112x^2 + 111x^3 + 434x^4 - 1050x^5 + 230x^6 + 823x^7 - 241x^8 - 9x^9 + 13x^{10} - 118x^{11} - 24x^{12}. \end{aligned}$$

## 5 Conclusion

We have derived long series for the generating function, radius of gyration and area-weighted moments of osculating and neighbour-avoiding polygons. Our extended series enables us to give precise estimate of the connective constants  $\mu^{\text{O}} = 2.677924128(5)$  for OP and  $\mu^{\text{NA}} = 2.315845(4)$  for NAP. As expected these values are, respectively, larger and smaller than the

connective constant for SAP. The exponent estimates are consistent with the exact values  $\alpha = 1/2$  and  $\nu = 3/4$ . We also obtain precise estimates for the leading amplitudes. Analysis of the coefficients of the radius of gyration series yielded results fully compatible with the prediction  $BD = 5/16\pi^2$  and from the first area-weighted moment we confirmed the universality of the amplitude ratio  $E^{(1)}/D$ .

In addition we used the series data to obtain the generating functions for convex and almost-convex OP and NAP. In all cases these are very similar to the corresponding generating functions for SAP.

## E-mail or WWW retrieval of series

The series for the various generating functions studied in this paper can be obtained via e-mail by sending a request to I.Jensen@ms.unimelb.edu.au or via the world wide web on the URL <http://www.ms.unimelb.edu.au/~iwan/> by following the instructions.

## 6 Acknowledgements

This work was supported by a Fellowship and grant from the Australian Research Council. Part of the calculations were performed on the facilities of VPAC and APAC.

## References

- [1] D. Bennett-Wood, I. G. Enting, D. S. Gaunt, A. J. Guttmann, J. L. Leask, A. L. Owczarek and S. G. Whittington, *J. Phys. A* **31**, 4725 (1998).
- [2] D. Bennett-Wood, J. L. Cardy, I. G. Enting, A. J. Guttmann and A. L. Owczarek, *Nucl. Phys. B* **528**, 533 (1998).
- [3] R. Brak and A. J. Guttmann, *J. Phys. A* **23**, 4581 (1990).
- [4] J. L. Cardy, *Nucl. Phys. B* **419**, 411 (1994).
- [5] J. L. Cardy and A. J. Guttmann, *J. Phys. A* **26**, 2485 (1993).
- [6] A. R. Conway and A. J. Guttmann, *Phys. Rev. Lett.* **77**, 5284 (1996).
- [7] M. P. Delest and G. Viennot, *Theor. Comp. Sci.* **34**, 169 (1984).
- [8] I. G. Enting, *J. Phys. A* **13**, 3713 (1980).
- [9] I. G. Enting and A. J. Guttmann, *J. Phys. A* **18**, 1007 (1985).
- [10] I. G. Enting and A. J. Guttmann, *J. Phys. A* **22**, 1371 (1989).
- [11] I. G. Enting and A. J. Guttmann, *J. Stat. Phys.* **58**, 475 (1990).
- [12] I. G. Enting, A. J. Guttmann, L. B. Richmond and N. C. Wormald, *Random Structures and Algorithms* **3**, 445 (1992).

- [13] A. J. Guttmann and I. G. Enting, *J. Phys. A.* **21**, L165 (1988).
- [14] A. J. Guttmann and I. G. Enting, *J. Phys. A.* **21**, L467 (1988).
- [15] A. J. Guttmann, in *Phase Transitions and Critical Phenomena*, Vol. 13, eds. C Domb and J L Lebowitz, Academic Press, New York (1989).
- [16] B. D. Hughes, in *Random walks and random environments, Vol. I Random walks*, Clarendon Press, Oxford (1995).
- [17] I. Jensen and A. J. Guttmann, *J. Phys. A.* **31**, 8137 (1998).
- [18] I. Jensen and A. J. Guttmann, *J. Phys. A.* **32**, 4867 (1999).
- [19] I. Jensen, *J. Phys. A.* **33**, 3533 (2000).
- [20] D. Kim, *Discrete Math.* **70**, 47 (1988).
- [21] K. Y. Lin and S. J. Chang, *J. Phys. A.* **21**, 2635 (1988).
- [22] K. Y. Lin and W. J. Tzeng, *Int. J. Mod. Phys. B***5**, 1913 and 2551 (1991).
- [23] K. Y. Lin, *J. Phys. A.* **25**, 1835 (1992).
- [24] K. Y. Lin and S.-J. Lue, *Physica A* **270**, 453 (1999).
- [25] B. Nienhuis, *Phys. Rev. Letts.* **49**, 1062 (1982).
- [26] G. Pólya, *J. Comb. Theor.* **6**, 102 (1969).
- [27] V. Privman and J. Rudnick, *J. Phys. A.* **18**, L789 (1985).
- [28] H. N. V. Temperley, *Phys. Rev.* **103**, 1 (1956).

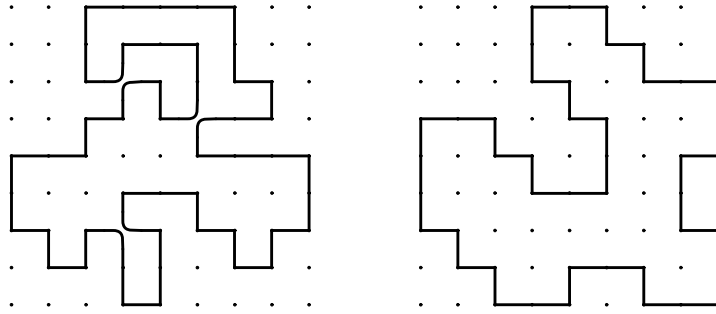


Figure 1: An example of an osculating polygon (left panel) and a neighbour-avoiding polygon (right panel).

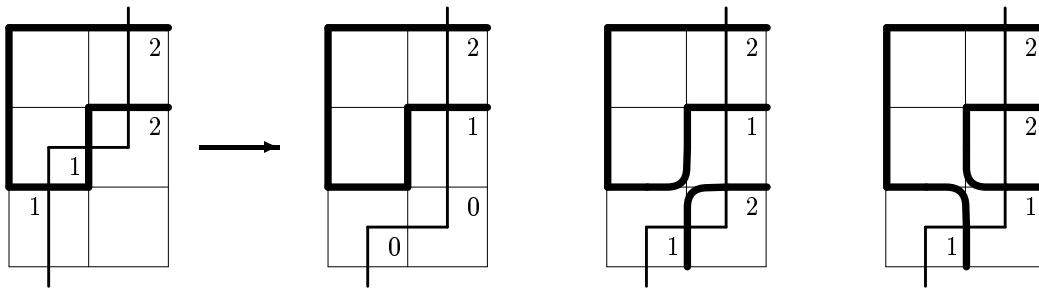


Figure 2: The input state  $\{01122\}$  and the three possible output states,  $\{00012\}$  where the lower ends are joined with no further action,  $\{01212\}$  where the lower ends are joined and a new loop is inserted, and  $\{01122\}$  where the lower ends ‘bounce’ of one-another.

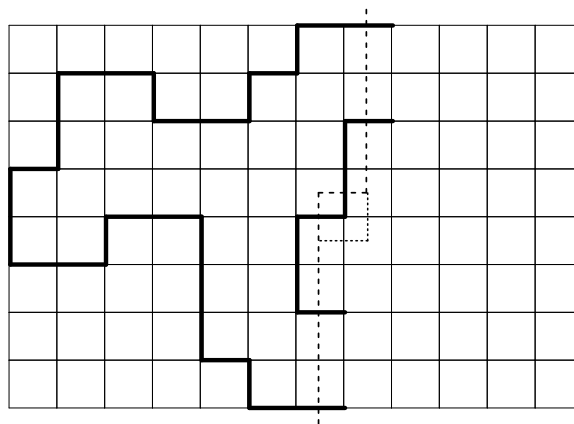


Figure 3: A snapshot of the boundary line during the transfer-matrix calculation for polygons.

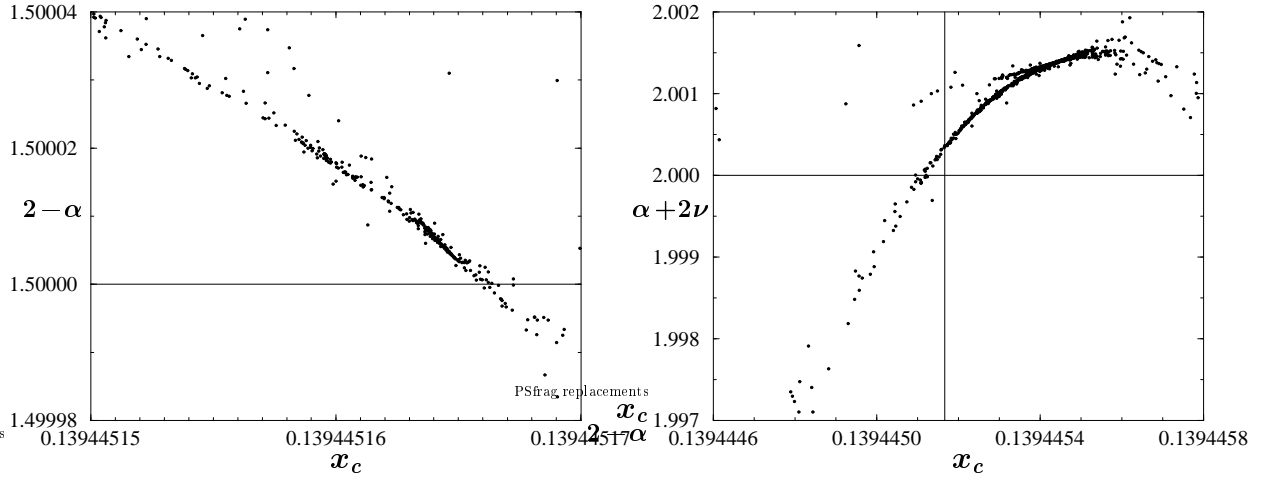


Figure 4: Estimates for the critical exponent  $2 - \alpha$  (left panel) and  $\alpha + 2\nu$  (right panel) vs. the corresponding estimates for critical point  $x_c$  as obtained from third order differential approximants to the OP generating function and radius of gyration series. The horizontal lines indicate the expected exponent values while the vertical line in the right panel indicates the estimate for  $x_c$  obtained from the data in the left panel.

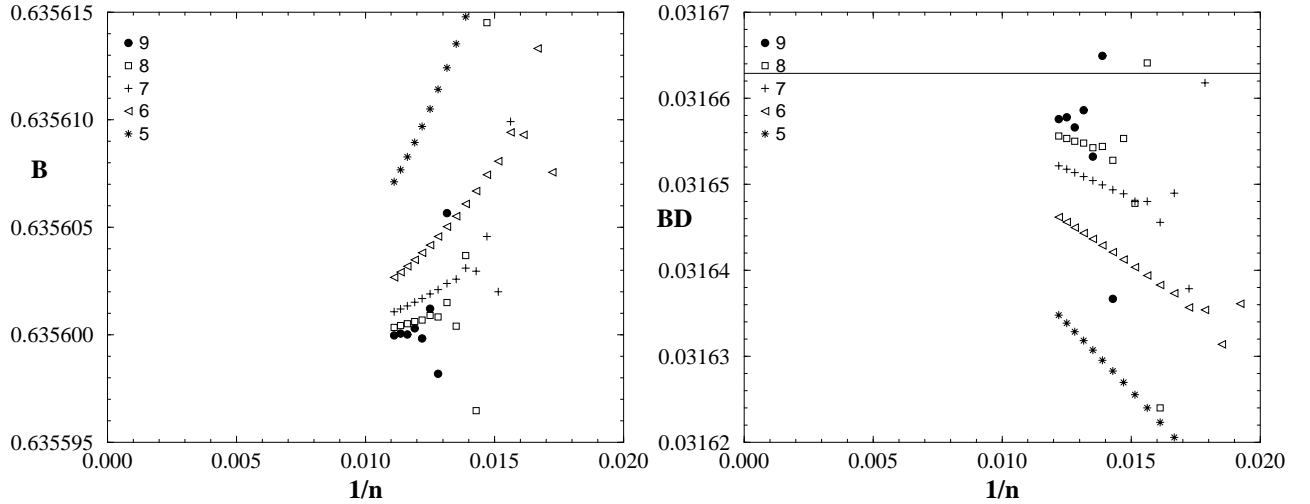


Figure 5: Estimates for the leading amplitudes  $B$  (left panel) of the OP generating function and amplitude combination  $BD$  (right panel) from the radius of gyration series vs.  $1/n$ . In each case we show data using varying numbers of terms in the expansions in Eq. (6) and (7), respectively. The horizontal line in the second panel indicate the expected exact value of the amplitude combination  $BD$ .

Table 1: The updating rules for the transfer-matrix algorithm for osculating polygons. The new partial generating function is multiplied by a factor  $x^k$ , where  $k$  is the number of '1' and '2' entries in the local output state. States marked by over-lining indicates instances in which two loop-ends are joined and other edges have to be relabelled as described by Enting [8].

	0	1	2
0	00 12	01 10	02 20
1	01 10	<u>00 12</u> 11	acc <u>12</u>
2	02 20	00 12 21	<u>00 12</u> 22

Table 2: The updating rules for the transfer-matrix algorithm for neighbour avoiding polygons. Similar remarks as for OP apply. States marked with a \* are only created conditionally depending on the states of nearby edges and states marked – should never occur provided the conditional updating is implemented correctly.

	0	1	2	3
0	00 12*	13* 31*	23* 32	00
1	13 31	<u>33</u>	add	–
2	23* 32	33	<u>33</u>	–
3	00	–	–	00

Table 3: Estimates for the critical point  $x_c$  and exponents obtained from second order differential approximants to the series for generating function, the radius of gyration and first moments of area of square lattice osculating polygons.  $L$  is the order of the inhomogeneous polynomial.

Series:	$\mathcal{P}(u)$		$\mathcal{R}_q^2(u)$		$\mathcal{P}^{(1)}(u)$	
$L$	$x_c$	$\alpha$	$x_c$	$-(\alpha + 2\nu)$	$x_c$	$2 - (\alpha + 2\nu)$
Second order differential approximants						
0	0.1394451590(29)	1.5000193(66)	0.139445388(43)	-2.001275(91)	0.139445489(67)	-0.00113(18)
2	0.1394451653(12)	1.5000025(36)	0.139445384(53)	-2.00125(12)	0.139445339(72)	-0.00084(16)
4	0.1394451636(10)	1.5000073(29)	0.139445401(58)	-2.00128(13)	0.139445255(37)	-0.00061(46)
6	0.1394451625(30)	1.500012(12)	0.139445400(51)	-2.00129(10)	0.13944532(10)	-0.00075(27)
8	0.1394451629(25)	1.5000093(69)	0.139445391(46)	-2.001271(99)	0.139445276(82)	-0.00061(29)
10	0.1394451631(17)	1.5000092(52)	0.139445394(48)	-2.00127(10)	0.139445272(26)	-0.000642(98)
Third order differential approximants						
0	0.1394451623(29)	1.5000122(92)	0.139445384(71)	-2.00123(20)	0.13944529(10)	-0.00064(30)
2	0.1394451641(30)	1.5000061(78)	0.139445444(54)	-2.00138(12)	0.139445240(22)	-0.000485(63)
4	0.1394451621(24)	1.500014(10)	0.139445448(53)	-2.001381(78)	0.139445209(68)	-0.00036(25)
6	0.1394451628(20)	1.5000100(54)	0.139445397(69)	-2.00126(19)	0.139445252(39)	-0.00053(13)
8	0.1394451637(10)	1.5000078(37)	0.139445433(18)	-2.001367(36)	0.139445212(50)	-0.00037(21)
10	0.1394451640(18)	1.5000062(60)	0.13944541(13)	-2.00118(45)	0.139445272(83)	-0.00056(23)

Table 4: Estimates for the critical point  $x_c$  and exponents obtained from second order differential approximants to the series for generating function, the radius of gyration and first moments of area of square lattice neighbour-avoiding polygons.  $L$  is the order of the inhomogeneous polynomial.

Series:	$\mathcal{P}(u)$		$\mathcal{R}_q^2(u)$		$\mathcal{P}^{(1)}(u)$	
$L$	$x_c$	$\alpha$	$x_c$	$-(\alpha + 2\nu)$	$x_c$	$2 - (\alpha + 2\nu)$
Second order differential approximants						
0	0.1864560(16)	1.5026(17)	0.186403(12)	-1.9453(65)	0.186424(31)	0.037(28)
2	0.1864551(25)	1.5033(30)	0.186429(11)	-1.9602(88)	0.1864488(42)	0.0130(48)
4	0.1864532(56)	1.5043(68)	0.186433(14)	-1.962(11)	0.1864485(74)	0.0133(84)
6	0.1864538(16)	1.5049(17)	0.186425(11)	-1.9566(70)	0.186448(12)	0.011(14)
8	0.1864555(29)	1.5030(32)	0.186426(13)	-1.9581(96)	0.186445(11)	0.016(11)
10	0.1864527(63)	1.5046(64)	0.1864312(84)	-1.9605(70)	0.1864533(64)	0.0070(74)
Third order differential approximants						
0	0.1864567(30)	1.5011(39)	0.186442(28)	-1.983(32)	0.186446(10)	0.0155(99)
2	0.1864572(13)	1.5011(16)	0.186416(43)	-1.960(39)	0.1864505(56)	0.0113(56)
4	0.1864573(22)	1.5007(30)	0.186447(20)	-1.975(47)	0.186449(11)	0.010(13)
6	0.1864563(22)	1.5020(27)	0.1864493(79)	-1.9872(96)	0.1864513(44)	0.0097(45)
8	0.1864568(40)	1.5006(60)	0.186450(13)	-1.988(18)	0.186437(25)	0.022(29)
10	0.1864550(37)	1.5037(44)	0.186461(19)	-2.005(28)	0.186439(24)	0.024(32)